MECHANICAL CHARACTERIZATION OF MULTICRYSTALLINE SILICON SUBSTRATES FOR SOLAR CELL APPLICATIONS

E.M. Tejado[1], T. Orellana[2], J.Y. Pastor[1], C. Funke[3], W. Fütterer[3]

[1]Departamento de Ciencia de Materiales-CISDEM, Universidad Politécnica de Madrid,
E.T.S. de Ingenieros de Caminos, Canales y Puertos 28040 Madrid, Spain
E-mail: elena.tejado@mater.upm.es

[2]Fraunhofer Institute for Solar Energy Systems, Heidenhofstrasse 2, 79110 Freiburg, Germany

[3]Institute for Experimental Physics, TU Bergakademie, Leipziger Strasse 23, D-09599 Freiberg, Germany

RESUMEN

La posibilidad de utilizar como materia prima silicio de menor pureza en la producción de células solares, como por ejemplo en sustratos para equivalentes de oblea epitaxiales, es de interés cuando la reducción de costes y las propiedades obtenidas resultan atractivas. En este trabajo se han analizado las propiedades mecánicas de dos bloques de silicio metalúrgico (UMG-Si), conocido por elevada concentración de impurezas respecto del silicio de alto grado, lo que puede reducir la resistencia mecánica de las obleas y limitar su uso comercial. Estas impurezas son principalmente aluminio y compuestos de silicio. Por tanto, a fin de lograr altos rendimientos de producción, es importante cuantificar su impacto en el comportamiento mecánico del UMG-Si. Esta caracterización mecánica consistió en la determinación del módulo de elasticidad, la resistencia mecánica y la tenacidad de fractura de las muestras. Para la obtención de la resistencia mecánica se rompieron las obleas bajo las condiciones del ensayo de flexión a tres puntos (TPB) y anillos concéntricos (ROR). Adicionalmente, mediante microscopía óptica y electrónica de barrido, se han examinado las superficies de fractura y la microestructura de las obleas estudiadas. Los resultados muestran que las impurezas con valores de tenacidad superiores a los del silicio pueden aumentar la resistencia mecánica de las obleas, constituyendo en muchos casos un obstáculo para la propagación de grietas. Por otro lado, las mismas impurezas pueden ser iniciadoras de la fractura, debido a las tensiones térmicas residuales introducidas durante el proceso de cristalización.

ABSTRACT

The possibility of using more economical silicon feedstock, i.e. as support for epitaxial solar cells, is of interest when the cost reduction and the properties are attractive. We have investigated the mechanical behaviour of two blocks of upgraded metallurgical silicon, which is known to present high content of impurities even after being purified by the directional solidification process. These impurities are mainly metals like Al and silicon compounds. Thus, it is important to characterize their effect in order to improve cell performance and to ensure the survival of the wafers throughout the solar value chain. Microstructure and mechanical properties were studied by means of ring on ring and three point bending tests. Additionally, elastic modulus and fracture toughness were measured. These results showed that it is possible to obtain marked improvements in toughness when impurities act as microscopic internal crack arrestors. However, the same impurities can be initiators of damage due to residual thermal stresses introduced during the crystallization process.

PALABRAS CLAVE: Comportamiento mecánico, silicio policristalino, efecto de la microestructura.

1. INTRODUCTION

Upgraded metallurgical grade silicon (UMG-Si) is particularly interesting for the photovoltaic industry as an attractive low-cost material for Si solar cell applications [1].

However, performance of UMG-Si solar cells largely depends on transport properties dominated by impurities and grain boundaries [2]. Consequently, other routes are being explored to face the lack of solar grade silicon and to reduce the payback time of this technology (the time during which the solar cell produces the same amount of energy that was used to create it) [3].

Among the different routes that are being explored, the epitaxial thin-film concept promises to reduce the cost for photovoltaic solar energy conversion [4]. In this technology, a high quality Si layer is deposited epitaxially on a low-cost Si substrate (e.g. cast Upgraded Metallurgical Grade silicon or high-throughput Si ribbons) and processed into a solar cell. This technology combines the well-known advantages of crystalline Si (high efficiency potential, stability and reliability) with a substantial cost reduction potential, as most of the Si material merely acts as a mechanical carrier for the solar cell device with most of the optical absorption taking place in the upper 30 µm [5].

Additionally, developing best quality and less expensive mc-Si cells can also be achieved by reducing the wafers thickness and by recycling silicon from silicon containing waste. Both strategies require exhaustive researches about the effect of the higher concentration of impurities on the mechanical properties of the substrate, in order to obtain high solar cell efficiencies and module production.

To establish this relationship, mechanical tests are necessary. Therefore the aims of this paper are twofold. First, it will study the impact of most common impurities on the mechanical behavior of mc-Si wafer with a view to identifying their effect on the strength of the substrate. While the second aim of the paper is to compare the results obtained for the two test configurations performed in order to determine the flexural strength of the specimens: Three Points Bending (TPB) and Ring On Ring tests (ROR).

2. EXPERIMENTAL PROCEDURE

The initial material was upgraded metallurgical silicon, so called UMG-Si, crystallized by the Fraunhofer ISE with the Vertical Gradient Freeze method into two blocks. Details of the process have already been published [6]. This material is characterized by high concentration of impurities whose mean values, evaluated by inductively coupled plasma optical emission spectrometry (ICP-OES) are given in Table 1.

Table 1. Concentration of impurities in Blocks 7 and 8 [ppmw] [7]

Impurity	Al	B	Ca	Cu	Fe	Mn
Block 7	217	177	669	4	370	46
Block 8	3634	36	13	2	18	1

In order to tackle the present study, samples from the bottom, the central part, and the top part of the two UMG-Si ingots were collected for mechanical characterization. Specimens were cut from the UMG-Si block and sliced with the multi-wire slurry saw into 270 µm and 2 mm thick wafers for ROR and TPB, respectively. To remove any subsurface damage, wafers were etched with an acidic aqueous chemical solution and a silicon layer of approximately 10-15 µm was etched per side of the wafer.

2.1. Ring on ring test

In order to perform equibiaxial tests, as-cut, etched and annealed UMG-Si substrates were diced with a laser into round silicon chips of 270 um thickness. The material testing machine DO-FB0.5TS (Zwick/Roell Company) was used with a ring on ring test configuration manufactured under the specifications of the ASTM C 1499 standard [8].

From the measured force-displacement curves the maximum principle stresses at which the wafers broke were calculated. For this purpose the TU Bergakademie Freiberg used the Finite Element program Ansys. Finally, data obtained from the flexural tests were submitted to Weibull statistics analysis to obtain the shape (m) and scale parameters of the different materials [9]. For this purpose, the characteristic stress is considered to be a representative value for the mechanical strength of the group of wafers tested, while the numerical value of *m* accounts for the dispersion of resistance values and thus the homogeneity of the samples analyzed.

2.2. Three-point bend test

The flexural strengths of the specimens were also determined using the three-point bending test as per ASTM C 1161-02C [10]. Specimens (initial probes dimensions: 69 x 8 x 9,78 mm) were tested with a spam length of 10 mm at room temperature and pressure using an instrumented 1 ton capacity Instron 5866 testing machine (Instron Limited, USA). Each sample was compressed with a constant speed of 100 µm/min.

Since in all cases the material presented a linear and elastic behavior until failure, ultimate stress was defined as stress at breaking force, using afterwards the Weibull statistical model. Tensile fracture stresses, σ_f were calculated with the equations of the linear fracture theory (1):

$$\sigma_f = \frac{3PL}{2BD^2} \qquad (1)$$

Where P is the measured load at failure and L, B and D are the span distance, breadth and height of the prismatic test pieces.

2.3. Fracture toughness

The fracture toughness was measured by the conventional single-edge-notched beam (SENB) method. Three-point tests, with 10 mm span, were conducted for the accurate determination of fracture toughness, as seen in Figure 1. To determine this mechanical property, a straight notch of around 130 µm was cut with a very thin diamond wire. The notch root radius was measured using a profile projector with an enlargement of 50×. The nominal notch depth was approximately 35% the specimen depth. This type of measurement is relevant because there are no measured values of toughness of mc-Si, containing different types of impurities, in the literature.

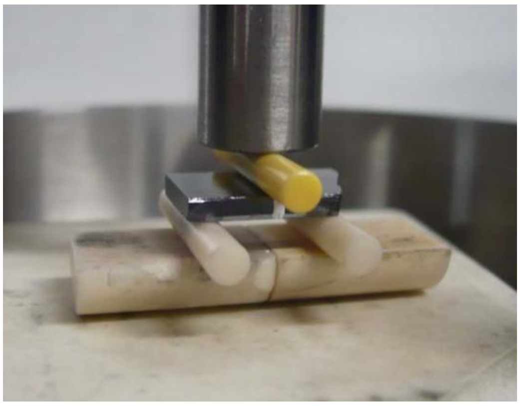

Figure 1. Three point bending test single edge notch beam test configuration.

Finally, the fracture toughness was computed from the failure load and the rod section using the stress intensity factor supplied by Guinea *et al*. [11].

2.4. Fracture surface analysis

Additional information was obtained with morphological (SEM) and chemical (EDS and XPS) surface analyses in a JEOL-JSM-6300 scanning electron microscope.

Prior to the fragmentation study, the samples were cleaned using ultrasonic waves in acetone. Local chemical analysis of the material was made by X-ray microanalysis, using the EDX spectrometer.

3. RESULTS AND DISCUSSIONS

3.1. Flexural strength

The Weibull modulus *m*, describes the variability of strength data. The higher the value of the Weibull modulus, the smaller is the scattering of the measured strengths. By plotting In (−In(1−F)) versus In(σ), a linear fit allows the calculation of the characteristic strength and the Weibull modulus. The experimental data can be fitted using a Weibull plot. For all cases, these distributions presented unimodal probability distribution behaviour as material failure is due to a single family of surface defects [12]. The Weibull parameters obtained for both Blocks against the relative position of the samples are summarized in Figure 2.

The relative positions in the blocks, “bottom”, “middle” and “top” are designated with the numbers “0”, “0,5” and “1” respectively. This nomenclature is valid for all graphs in this paper.

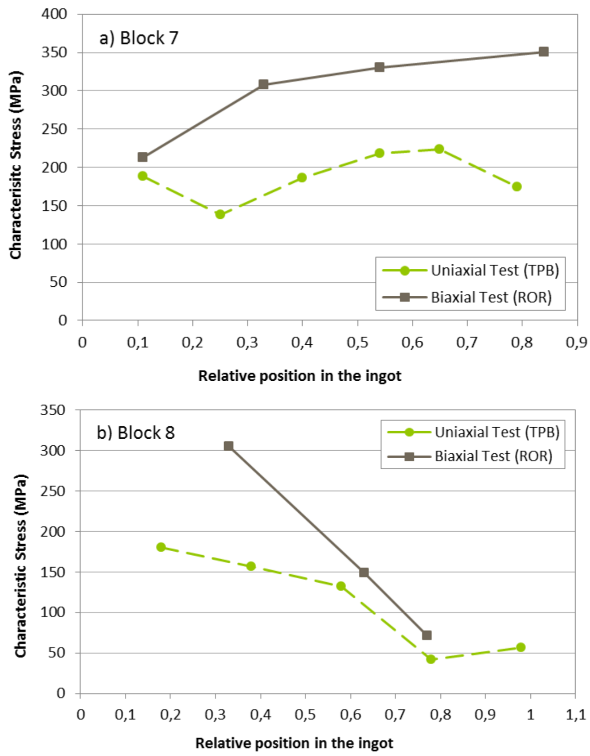

Figure 2. Statistical breakage rate of UMG-Si wafers obtained with both bending techniques. a) Block 7 b) Block 8

There were significant differences between the two blocks evaluated, either for the three-point or the ring-on-ring test configurations. In fact, while flexural strength of the Block 7 was higher for bottom wafers than for the top ones, the second Block analyzed shows the opposite behavior. The highest values obtained for the wafers collected from the bottom part of Block 8 correspond to those obtained for the highest position of the Block 7, as there is a high concentration of Si_3N_4 and SiC precipitates in these areas. However, due to the microcracks that originate Al_2O_3 and aluminum precipitates in the upper regions of Block 8, the mechanical strength decreases dramatically.

When comparing both bending techniques, a significantly higher flexural strength with the ring on ring bending test was observed for both blocks, which corroborate the existing literature referred to the volume of the specimen that is effectively under stress and its probability of failure [13]. For biaxial tests, as the area subjected to stress is higher, fracture probability curves present a broader Weibull distribution [14]. Furthermore, there is another aspect that might explain this finding: the presence of edge flaws facilitates crack initiation in uniaxial tests, reducing specimen strength [15]. In biaxial specimens, the presence of edge flaws does not have such an influence, since the disk edges are located in a low stress area.

3.2. Fracture toughness

The fracture toughness (mean value and standard error) of the wafers from the two blocks analyzed are summarized in Table 2.

Table 2. Results of fracture toughness tests on blocks of study.

Block 7			Block 8		
Position	**K_{IC} (MPa m$^{1/2}$)**	**$\sigma_{\bar{x}}$**	**Position**	**K_{IC} (MPa m$^{1/2}$)**	**$\sigma_{\bar{x}}$**
1	1,46	0,07	1	1,38	0,21
2	1,25	0,05	2	1,43	0,15
3	1,29	0,05	3	1,61	0,20
4	1,55	0,14	4	1,27	0,32
5	1,57	0,17	-	-	-
6	1,33	0,18	5	1,34	0,19

Both materials exhibit the same tendency, ie, toughness increases as the height in the block increases, reaching a maximum at around 65% of the total height in which the values decrease again. This could be due to the greater cleanliness of these areas of the blocks, as impurities segregate to the bottom of the block, or are rather dissolved in the liquid layer or sink.

Fracture surface analysis of sample was combined with fracture mechanics relationships as a quantitative tool in order to determine the toughness of the material. Nevertheless fractographic analysis of the UMG-Si was not straightforward as fracture surfaces were usually rough and irregular making unequivocal identification of the origin challenging.

In brittle materials such as ceramics, fracture begins from a single location called the fracture origin, which is a discontinuity such as a flaw or a defect that has developed from mechanical, chemical or thermal processes that will act as a localized stress concentrator. These sharp cracks are visible on the fracture surface and their semi-elliptical dimensions enable K_{IC} to be calculated using fracture mechanics analysis for surface flaws in bending. The conventional equation for fracture toughness calculation for small flaws in tensile fields [16] is:

$$K_{IC} = Y \times \sigma_{max} \times \sqrt{c} \qquad (2)$$

where c is the crack depth , σ_{max}, the fracture stress at the origin (MPa) and Y the dimensionless stress intensity shape factor whose value is 1.98.

This study was carried out on several samples. So that, for a wafer collected from the middle position of the Block 7 with a tensile strength of 138.01 MPa and whose fracture toughness is 1.25 MPa m$^{1/2}$, the critical semi-elliptic defect size is approximately 50 microns, as shown in Figure 5.

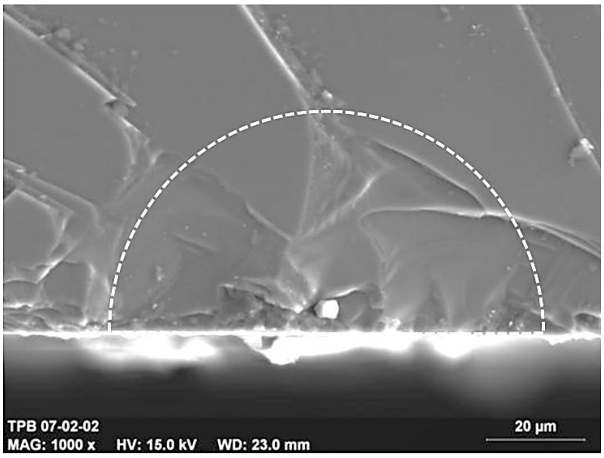

Figure 3. SEM image of the fracture origin. Block 8.

The approximated dimension of the critical defect has been highlighted according to equation 2. As shown, despite the complex fractography shown in the fracture surface of these materials an acceptable approximation can be achieved.

3.3. Fractographic analysis

The analysis of the fractured surface allowed the observation of fractographic features commonly found in brittle specimens. For all samples, fractured surfaces fit perfectly with no signs of macroscopic plastic deformation. Also in all cases, the fractographical analysis revealed that fracture origin was located on the surface opposed to the central loading point on the side of the samples under tensile stress.

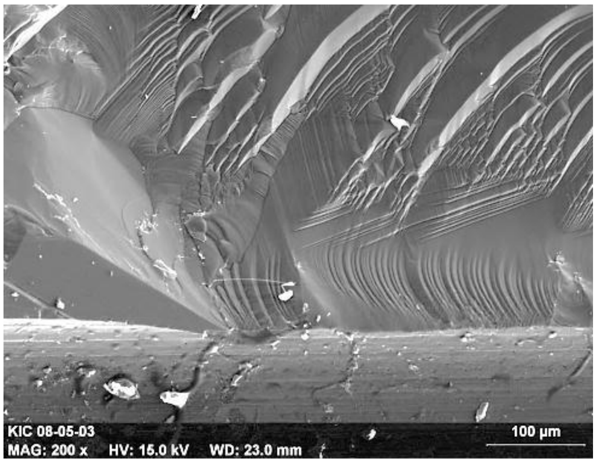

Figure 4. SEM image of the fracture surfaces of the top part of Block 8.

Figure 4 shows the surrounding area to the notch introduced, with characteristic river marks of a transgranular fracture.

After analyzing the imagines various impurities have been encountered:

- *Aluminum*

Block 7 had a high content of Al (3634 ppmw) as indicated in the Experimental Procedure. The presence of this metal in the silicon matrix was also determined by SEM analysis. As obtained from TPB and ROR tests results, Al was the most detrimental type of impurity for the mechanical strength of mc-Si wafers, which is in good agreement with previous literature data. Aluminum has a thermal expansion coefficient of 24×10-6 K^{-1} while silicon has a coefficient of 4.3×10-6 K^{-1}, this difference is the responsible of the very high thermal residual stresses which cause the microcracking of the silicon matrix, as seen in Figure 5.

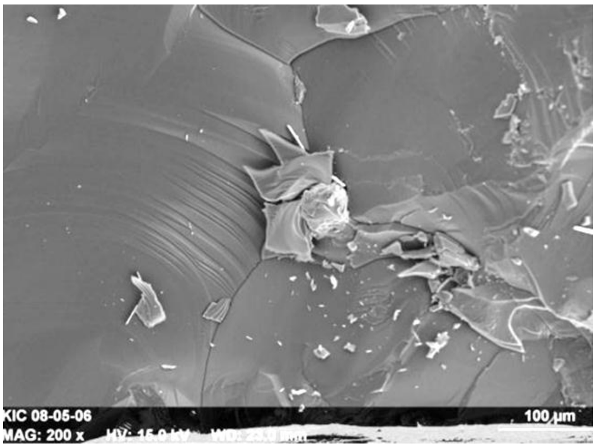

Figure 5. SEM image of microcracks formed in the surroundings of aluminum particles in the silicon matrix.

- *Silicon Oxide*

This compound precipitated mainly in the lowest areas of Block 7 as crystalline and amorphous inclusions (see Figure 6). In this case, the differences between the coefficients of thermal expansion are not as significant as in the previous case (the coefficient of thermal expansion of amorphous SiO_2 is 0.5x10.6 K^{-1} versus 4.3x 10.6 K^{-1} which exhibits the crystalline silicon), so that there was no such abundance of microcracks in the surroundings of SiO_2 particles. Furthermore, the size of the inclusions is significantly lower than aluminum ones. Moreover, SiO_2 particles do not show toughening effect on the silicon matrix.

- *Silicon carbide*

SiC particles present in the upper parts of the mc-Si blocks decrease the mechanical strength of wafers due to the overlap of radial thermal stresses caused by thermal and elastic mismatch.

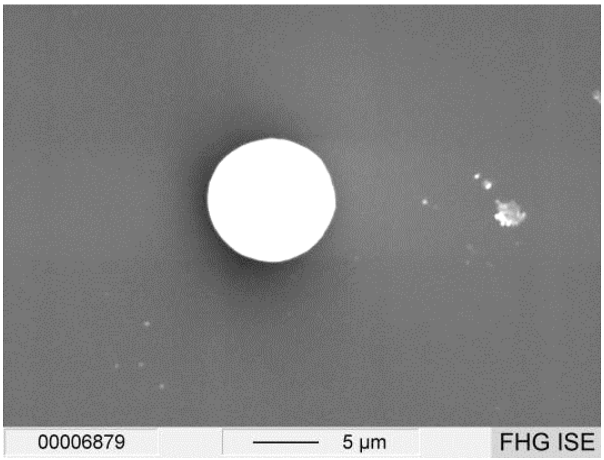

Figure 6. SEM image of SiO_2 particles in the silicon matrix.

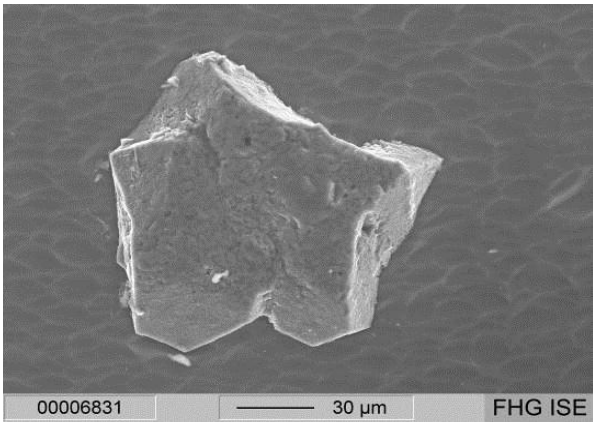

Figure 7. SEM image of a SiC particle in the silicon matrix.

However, the value of toughness corresponding to samples tested at 73% of the relative ingot height is 1.75±0.42 MPa $m^{1/2}$. As the toughness of the SiC particles, 3.0 MPa $m^{1/2}$, is higher than the one of single crystal silicon, 0.9 MPa $m^{1/2}$, SiC can be responsible for this significant increase in toughness of mc-Si, which counteract partially the decrease in mechanical strength.

- *Silicon nitride*

In the upper parts of the silicon blocks Si_3N_4 precipitates together with SiC particles. Scanning microscope inspection did not reveal this type of impurity particles as fracture initiators but as obstacles in the propagation of cracks as these particles are well bonded to the silicon matrix. Si_3N_4 exhibits a fracture toughness that varies between 4.0 MPa $m^{1/2}$ and 6.1 MPa $m^{1/2}$, is very well bonded with the silicon matrix, and its geometry makes it difficult for the crack to surround the particle. Thus, the crack can only break through the Si_3N_4 particle to continue its propagation, which requires an extra consumption of energy (see Fig. 8). This fact is the responsible for the toughening capacity of Si_3N_4 particles.

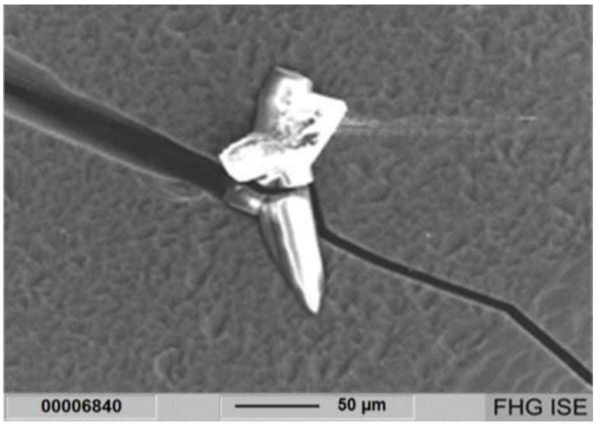

Figure 8. SEM image of a Si_3N_4 particle in the silicon matrix.

4. CONCLUSIONS

According to the results and subsequent discussion, the following conclusions can be obtained:

- Mechanical properties of two blocks of metallurgical grade silicon crystallized by directional solidification technique have been studied. Fracture toughness and flexural strength of metallurgical silicon samples have been obtained in a reproducible manner, which is very interesting as there is very little data in the literature for these materials.

- Results obtained from equibiaxial and uniaxial tests have been compared, being consistent with existing literature.

- The location of the impurities in the blocks is regulated by the law of Scheils, whereby the Block 7 concentrates most of the impurities of SiO2 in the lower zone, while SiC and Si_3N_4 impurities are concentrated in the upper parts of this block. Otherwise, in Block 8 the segregation coefficient of aluminum produces it segregation to the upper part of the block, as it is solved in the liquid layer to the end of solidification.

After analysis of the results, the influence of impurities on the mechanical properties of metallurgical silicon revealed that:

- The presence of metals, particularly aluminum, negatively affects the mechanical properties of the metallurgical silicon substrates. Introducing residual thermal stresses causing microcracks in the silicon matrix.
- The impurities of SiC and SiO 2 decreases the mechanical strength of the substrate, due to thermal stresses introduced during the solidification process.
- On the other hand, SiC and Si_3N_4 inclusions increase the toughness of the acting as microscopic internal crack arrestors.

Finally, fractographic analysis revealed multiple patterns of crack tortuosity, fragmentation and presence of relief, a process associated with brittle fracture.

ACKNOWLEDGEMENTS

The authors gratefully acknowledge the financial support from the *Spanish Ministry for the Economy and Competitiveness* (Projects CSD00C-06-14102 and MAT2009-13979-C03-02 and by a PhD *grant JAE*-Pre, CSIC), the *Community of Madrid* (S2009/MAT-1585-ESTRUMAT2) and the *Fraunhofer Society* (Project Si-Beacon).

REFERENCES

[1] S. De Wolf, J. Szlufcik, Y. Delannoy, I. Perichaud, C. Habler, R. Einhaus, *Solar cells from upgraded metallurgical grade (UMG) and plasma-purified UMG multicrystalline silicon substrates*, Sol. Energy Mater. Sol. Cells 72 (2002) 49–58.

[2] Hyo SikChang, *Effect of passivation process in upgraded metallurgical grade (UMG)-silicon solar cells,* Solar Energy Materials & Solar Cells 95 (2011) 63–65.

[3] E. Øvrelid, B. Geerligs, A.Wærnes, O. Raaness, I. Solheim, R. Jensen, K.Tang, S.Santeen, B. Wiersma, *Solar Grade Silicon by a Direct Metallurgical Process*, Silicon for the Chemical Industry VIII, Norway, 2006

[4] Sergio Pizzini, *Towards solar grade silicon: Challenges and benefits for low cost photovoltaics,* Solar Energy Materials & Solar Cells 94 (2010) 1528–1533.

[5] G. Beaucarne, F. Duerinckx, I. Kuzma, K. Van Nieuwenhuysen, H.J. Kim, J. Poortmans, *Epitaxial thin-film Si solar cells,* Thin Solid Films 511 – 512 (2006) 533 – 542.

[6] T. Orellana Pérez, C. Funke, W. Fütterer, T. Wagner, S. Riepe, S. Reber, H. J. Möller, *Mechanical characterization of epitaxial wafer equivalents from block casting to thin film deposition,* 2010.

[7] T. Orellana Pérez, C. Funke, W. Fütterer, S. Riepe, H. J. Möller, E. M. Tejado Garrido, J. Y. Pastor Caño, *Impact of impurities on the mechanical strength of multicrystalline silicon,* 26th European

Photovoltaic Solar Energy Conference and Exhibition

[8] ASTM C 1499, *Standard Test Method for Monotonic Equibiaxial Flexural Strength of Advanced Ceramics at Ambient Temperature*, 2008.

[9] ASTM C 1239-07, "*Standard Practice for Reporting Uniaxial Strength Data and Estimating Weibull Distribution Parameters for Advanced Ceramic*s", 2007.

[10] ASTM C 1161-02c, "*Standard Test Method for Flexural Strength of Advanced Ceramics at Ambient Temperature*", 2008

[11] G.V. Guinea, J.Y. Pastor, J. Planas and M. Elices. *Stress Intensity factor, compliance and CMOD for a general three-point-bend beam*. International Journal of Fracture 83: 103-116, 1998.

[12] J. Pascual Cosp, A. J. Ramírez del Valle, J. Zapa tero Arenzana, J. C. Galiano Serrano. *Análisis estadístico de la resistencia mecánica de materiales cerámicos de mullita sometidos a diferentes ciclos de calentamiento*. Boletín de la Sociedad española de cerámica y vidrio.

[13] Jin J, Takahashi H, Iwasaki N. *Effect of test method on flexural strength of recent dental ceramics*. Dent Mater J 2004; 23:490–6.

[14] B. Picka, J.B.C. Meiraa, L. Driemeierb, R.R. Bragaa. *A critical view on biaxial and short-beam uniaxial flexural strength tests applied to resin composites using Weibull, fractographic and finite element analyses*. Dental materials 26 (2010) 83–90.

[15] Higgs WAJ, Lucksanasombool P, Higgs RJED, Swain MV. *Evaluating acrylic and glass-ionomer cement strength using the biaxial flexure test.* Biomaterials 2001; 22:1583–90.

[16] M. Tanaka, K. Higashida, H. Nakashima, H. Takagi and M. Fujiwara, *Orientation dependence of fracture toughness measured by indentation methods and its relation to surface energy in single crystal silicon.*